

This is the accepted manuscript made available via CHORUS. The article has been published as:

## Starting Flow Past an Airfoil and its Acquired Lift in a Superfluid

Seth Musser, Davide Proment, Miguel Onorato, and William T. M. Irvine

Phys. Rev. Lett. **123**, 154502 — Published 11 October 2019

DOI: [10.1103/PhysRevLett.123.154502](https://doi.org/10.1103/PhysRevLett.123.154502)

# Flying in a superfluid: starting flow past an airfoil

Seth Musser,<sup>1</sup> Davide Proment,<sup>2</sup> Miguel Onorato,<sup>3</sup> and William T.M. Irvine<sup>4</sup>

<sup>1</sup>*Department of Physics, University of Chicago, Chicago IL, 60637, USA \**

<sup>2</sup>*School of Mathematics, University of East Anglia, Norwich Research Park, NR47TJ Norwich, UK*

<sup>3</sup>*Dipartimento di Fisica, Università degli Studi di Torino and INFN, Via Pietro Giuria 1, 10125 Torino, Italy*

<sup>4</sup>*James Franck Institute and Enrico Fermi Institute,*

*Department of Physics, University of Chicago, Chicago IL, 60637, USA*

We investigate superfluid flow around an airfoil accelerated to a finite velocity from rest. Using simulations of the Gross–Pitaevskii equation we find striking similarities to viscous flows: from production of starting vortices to convergence of airfoil circulation onto a quantized version of the Kutta–Joukowski circulation. We predict the number of quantized vortices nucleated by a given foil via a phenomenological argument. We further find stall-like behavior governed by airfoil speed, not angle of attack, as in classical flows. Finally we analyze the lift and drag acting on the airfoil.

The development of flow around an airfoil, see sketch in Figure 1(a), is a textbook problem in fluid mechanics [1–3]. Describing this fundamental process has practical relevance since it provides a route to understanding the controlled production and release of vorticity from asymmetric structures. In viscous weakly compressible fluids, in the subsonic regime, this release occurs through a subtle interplay of inviscid and viscous dynamics.

To address the inviscid, incompressible and two-dimensional dynamics, one can use the celebrated conformal Joukowski transformation to relate the flow around an airfoil to the simpler flow past a cylinder. This makes it possible to readily derive a family of allowed flows, characterized by the value of the circulation  $\Gamma$  around the airfoil. All but one of these flows feature a singularity in the velocity at the trailing edge. To avoid this singularity, the Kutta–Joukowski condition prescribes a circulation,  $\Gamma_{KJ} = -\pi U_\infty L \sin(\alpha)$ , where  $L$  is the airfoil chord,  $U_\infty$  the speed and  $\alpha$  the angle of attack. It then follows that the airfoil experiences a lift force per unit of wingspan given by  $-\rho U_\infty \Gamma_{KJ}$  and will not experience any drag force.

A major issue with this inviscid theory is that the circulation  $\Gamma_{KJ}$  is prescribed by hand. Replacing the ideal fluid with an incompressible but viscous fluid and enforcing the no-slip boundary condition gives rise to a boundary layer where the velocity interpolates from zero, on the surface of the airfoil, to the potential velocity outside [1]. Far from the boundary layer, the flow remains similar to the inviscid case. As the trailing edge is approached, the high speeds create a pressure gradient that pulls the boundary layer off the airfoil and into a starting vortex, generating a circulation  $\Gamma_{KJ}$  around the airfoil (see Fig. 1(a)). Because the airfoil acquires the same circulation as in the ideal case, its lift remains unchanged, though the airfoil experiences a nonzero drag due to viscosity [1].

In this Letter we address the physics of flow past an airfoil in a superfluid. In particular, we ask whether (i) there exists a mechanism allowing for the generation of a circulation; if so, (ii) whether the Kutta–Joukowski condition

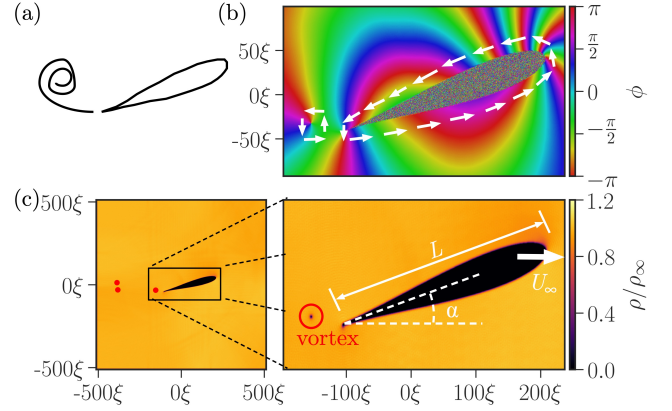


FIG. 1. Generation of circulation: (a) A cartoon showing the starting vortex produced in a viscous fluid. (b) The phase field around the airfoil potential. By counting phase jumps around the airfoil the value of the circulation can be obtained. A quantized vortex is visible behind the airfoil’s trailing edge. (c) Left hand - the density field in the full computational box. The density is rescaled by the superfluid bulk density, length scales are expressed in units of  $\xi$ , quantized vortices are shown as red dots. A closer view of airfoil is shown on the right. Relevant airfoil parameters are labeled and the vortex is circled in red.

holds and finally, (iii) whether the airfoil experiences lift and/or drag. In order to answer these questions we combine an analytical approach with numerical simulations. As a model for the superfluid, we consider the Gross–Pitaevskii equation (GPE) which has been successfully used to reproduce aspects of both inviscid and viscous flow, including: the shedding of vortices from a disk [4–7], an ellipse [8, 9], a sphere [10] and a cylinder [8, 11], the formation of Von Kármán vortex sheets [5, 12], the emergence of a superfluid boundary layer [13], the dynamics and decay of vortex loops and knots [14, 15], and the appearance of classical-like turbulent cascades [16, 17].

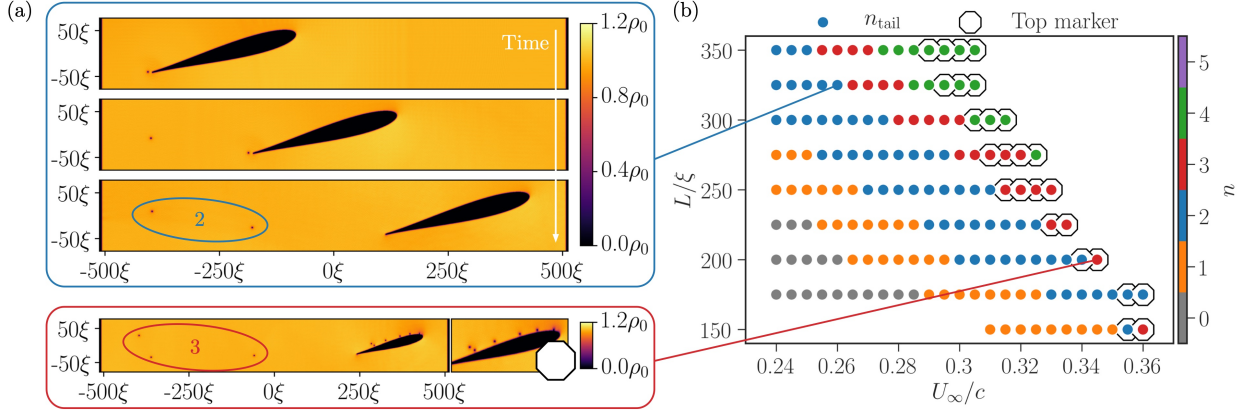


FIG. 2. Vortex emission: (a) Vortices nucleated at the tail and top of a Joukowski airfoil having  $\alpha = 15^\circ$ ,  $\tilde{\lambda} = 0.1$ . Here the width of the foil scales like  $\tilde{\lambda}L$  (see SI). The computational box size is  $1024\xi \times 1024\xi$ . Tail number reflected by color, top nucleation by octagon mark. (b) Top three frames are snapshots of the density field for  $U_\infty = 0.260c$  and  $L = 325\xi$ ; here  $n_{\text{tail}} = 2$ . Bottom frame has  $U_\infty = 0.345c$  and  $L = 200\xi$ . This foil nucleates thrice from tail before nucleating uncontrollably from top; right shows closer view of top vortices.

The two-dimensional GPE is:

$$i\hbar \frac{\partial \psi}{\partial t} = \left( -\frac{\hbar^2}{2m} \nabla^2 + V + g|\psi|^2 \right) \psi, \quad (1)$$

where  $\psi = \psi(x, y, t)$  is the wave-function of the superfluid,  $\hbar$  is the reduced Planck's constant,  $g$  is the effective two-dimensional two-body coupling between the bosons of mass  $m$  and  $V$  is an external potential. Relevant bulk quantities are the speed of sound  $c = \sqrt{g\rho_\infty/m}$  and the healing length  $\xi = \sqrt{\hbar^2/(2mg\rho_\infty)}$ , with  $\rho_\infty$  the superfluid number density at infinity. The healing length is the length-scale for the superfluid to recover its bulk density value away from an obstacle; the speed of sound is the speed of density/phase waves of scales larger than  $\xi$ .

To understand the superfluid's dynamics in terms of hydrodynamic variables, we make use of the Madelung transformation  $\psi = \sqrt{\rho}e^{i\phi}$ . This recasts the GPE into hydrodynamical equations for the conservation of mass:  $\frac{\partial \rho}{\partial t} + \nabla \cdot (\rho \mathbf{u}) = 0$  and momentum:

$$\frac{\partial \mathbf{u}}{\partial t} + (\mathbf{u} \cdot \nabla) \mathbf{u} = \nabla \left[ -\frac{g}{m} \rho + \frac{1}{m} V + \frac{\hbar^2}{2m^2} \frac{\nabla^2 \sqrt{\rho}}{\sqrt{\rho}} \right], \quad (2)$$

where the density and the velocity of the superfluid are  $\rho = |\psi|^2$  and  $\mathbf{u} = (\hbar/m) \nabla \phi$ , respectively. These equations are equivalent to the barotropic Euler equations for an ideal fluid, with the exception of the presence of the quantum pressure term (the last in eq. (2)), negligible at scales larger than  $\xi$ . Circulation around a path  $C$  is given by  $\Gamma = \oint_C \mathbf{u} \cdot d\mathbf{l} = \hbar \Delta \phi / m$ , where  $\Delta \phi$  is the increment in  $\phi$  around  $C$ :  $\Delta \phi$  is quantized in units of  $2\pi$  and so is the circulation, in units  $\kappa = h/m$ . Quantized vortices are defined as those points for which the density is zero and the phase winds by  $2\pi$  around them. For example, a vortex can be seen in the phase field in Fig. 1(b); the same

vortex also appears circled in red in the density field of Fig. 1(c).

To mimic the motion of an airfoil we add a potential  $V = V[x(t), y]$  moving with velocity  $\dot{x}(t)$  along the  $x$  direction. Within the airfoil shape, the potential has a constant value fifty times higher than the superfluid chemical potential  $\mu = g\rho_\infty$ , and decays to zero within a healing length outside. At the beginning of each simulation the potential is accelerated up to a final velocity,  $U_\infty$  which is then kept constant. See SI (Supplementary Information) for details of the numerical scheme.

Soon after the airfoil is set into motion, a vortex is nucleated from the trailing edge, much like the starting vortex emitted in classical fluids. Our typical airfoil nucleates more than once; the bottom of Fig. 2(a) displays an example where three vortices are nucleated from its trailing edge. The number of vortices emitted depends in general on the airfoil's terminal velocity  $U_\infty$  and length  $L$ , as shown in Fig. 2(b). While most of the simulated airfoils reach a steady state post-nucleation, in some cases, highlighted with octagons in Fig. 2(b), the airfoil begins nucleating from its top after nucleating from the trailing edge. Once begun, nucleation from the top continues for the length of the simulation in a manner reminiscent of the stalling behaviour of a classical airfoil flow.

These results suggest that, just as for real fluids, an airfoil in a superfluid builds circulation by vortex emission from its trailing edge. A natural candidate for the mechanism underlying vortex emission is the onset of compressible effects at the tail of the foil [4, 7, 18]. To estimate this we consider an airfoil moving with constant terminal velocity  $U_\infty$ . At length scales larger than the healing length, quantum pressure is negligible and the problem simplifies to a classical inviscid compressible fluid one.

The usual condition of compressibility is that relative density variations must be larger than relative speed variations:  $|\nabla\rho|/\rho > |\nabla\cdot\mathbf{u}|/u$  [3]. In the steady flow and neglecting the quantum pressure, eq. (2) is nothing but the classical Bernoulli equation;  $\rho(u) = \rho_\infty + m(U_\infty^2 - u^2)/2g$ , where  $\rho_\infty$  is the far field density and  $U_\infty$  is the far field velocity in the foil's frame. Plugging  $\rho(u)$  into the compressibility condition, one obtains that compressibility effects arise when [19]:

$$\frac{3}{2} \frac{u^2}{c^2} - \frac{1}{2} \frac{U_\infty^2}{c^2} - 1 > 0, \quad (3)$$

i.e. when the local flow speed is greater than the *local* speed of sound. In classical fluids, a dissipative shock is formed where supersonic flow occurs. On the contrary, reaching the compressibility condition in numerous superfluid models leads to the shedding of vortices [7, 20, 21]. We use this phenomenological criterion to predict the number of vortices that will nucleate.

We proceed by approximating the velocity of the superfluid  $\mathbf{u}$  around the foil by the velocity of an ideal fluid,  $\mathbf{u}_{\text{ideal}}$ , around a Joukowski foil of length  $L$ , terminal velocity  $U_\infty$ , angle of attack  $\alpha$ , with a circulation  $\Gamma$ . See the SI for a comparison between this approximation and the simulated flow field. For a circulation  $\Gamma \neq \Gamma_{KJ}$ , the ideal flow speed  $|\mathbf{u}_{\text{ideal}}|$  increases sharply, eventually diverging as the sharp tail is approached. We expect this divergence to be cut-off by quantum pressure effects arising in the healing layer of size  $\xi$ . Following [22], we evaluate  $\mathbf{u}_{\text{ideal}}$  at a distance  $A\xi$ , where  $A$  is a factor of order unity, and predict vortex nucleation whenever the velocity exceeds the compressibility criterion of eq. (3). As vortices are nucleated, the value of  $\Gamma$  increments accordingly by  $\kappa$ . As  $\Gamma$  approaches  $\Gamma_{KJ}$  the speeds at the tail decrease and nucleation *from the tail* ends when enough vortices have been emitted to reduce speeds at the tail below the compressibility condition in eq. (3). We stress that, unlike periodic nucleation of oppositely signed vortices from symmetric obstacles as in [4, 6, 7, 10, 19, 23], all emitted vortices have the same sign. Figure 3(a) shows excellent agreement between our simulation data and this prediction for a value  $A \sim 0.55$ , close to the value 0.57 found by Rica et al [22] for a sharp corner.

As tail nucleation decreases the speed at the tail, the speed will increase over the top of the foil. Once an airfoil has finished nucleating from its tail, if ideal flow speeds at a distance of  $A\xi$  from the top are large enough to satisfy (3), then we predict the airfoil will stall by continuously emitting vortices from the top. The observed stall-like behavior is marked by octagons in Figure 3(a); its prediction is represented by the boundary of the colored area. This marks a radical difference between classical and superfluid flight: stalling in the superfluid is driven by the flow speed at the top of the foil. In viscous flow stalling is primarily a function of  $\alpha$ . See Figure 4 [24].

Returning to tail nucleation, we make our prediction of

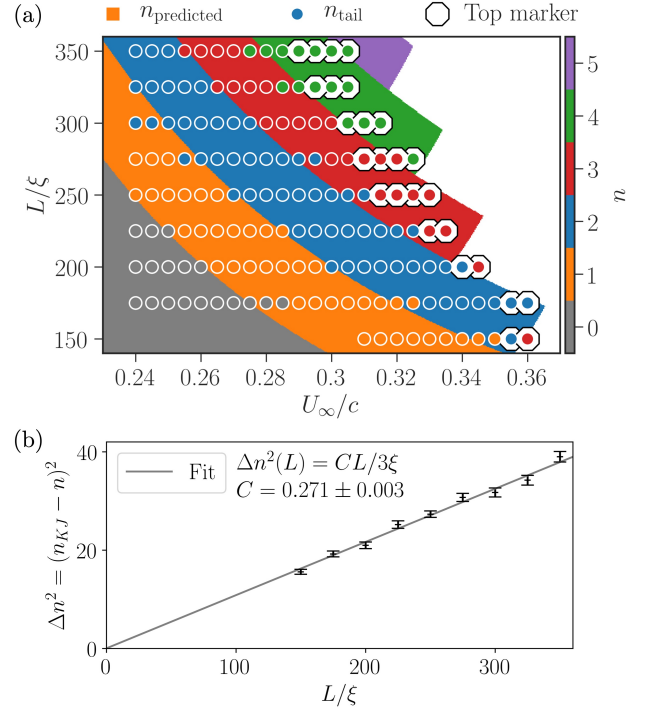


FIG. 3. Nucleation predictions: (a) Plot of tail and top nucleation numbers in  $U_\infty - L$  parameter space for  $\alpha = 15^\circ$ . Predictions are stripes in background, white area signifies predicted top nucleation. All predictions used a cut-off distance of  $A = 0.55\xi$  from the foil. Simulation data is circled in white. (b) Values of  $\Delta n^2$  calculated for each simulation in (a) with their average plotted vs.  $L/\xi$ . Errorbars are standard deviation of the mean for the  $U_\infty/c$  values in (a).

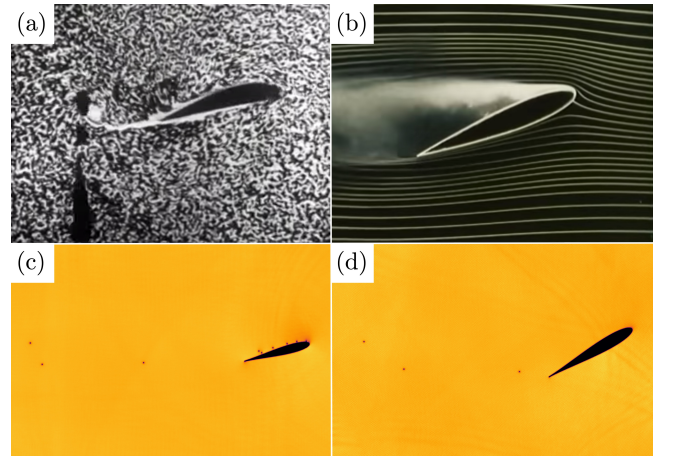


FIG. 4. Viscous vs. superfluid flight/stall: (a) Flight of foil in a viscous fluid at a low angle of attack. (b) Stall at high angle of attack. (c) Stall in a superfluid at low angle of attack. (d) Flight at high angle of attack.



nucleation number analytic by appealing to a Taylor expansion of  $\mathbf{u}_{\text{ideal}}$  at small distance from the tail. Solving the implicit equation (3) for  $\Gamma = n\kappa$ , reveals that

$$(\Gamma_{KJ}/\kappa - n)^2 \approx C(\alpha)L/(3\xi) \quad (4)$$

to first order [25] (See SI for details). Here  $C$  is a constant of order one whose value depends on the angle of attack  $\alpha$ . If we define  $n_{KJ} \equiv \Gamma_{KJ}/\kappa$  to be the number of vortices the foil would nucleate if it acquired a classical circulation, we obtain  $\Delta n^2 \equiv (n_{KJ} - n)^2 = C(\alpha)L/3\xi$ . We verify this linear relationship by plotting  $\Delta n^2$  vs.  $L/\xi$  for our simulations, and find excellent agreement shown in Figure 3(b).

Having understood the vortex nucleation, we turn our attention to the force experienced during this process, namely the lift and drag. The similarity of classical and superfluid vortex nucleation leads us to suspect that an airfoil's lift in a superfluid will be similar to that in a classical fluid, and thus that the Kutta–Joukowski Lift Theorem will nearly hold in a superfluid. To calculate the  $k$ th component of the force exerted by the superfluid on the airfoil one can integrate the stress-energy tensor

$$T_{jk} = m\rho u_j u_k + \frac{1}{2}\delta_{jk}g\rho^2 - \frac{\hbar^2}{4m}\rho\partial_j\partial_k\ln\rho \quad (5)$$

around any path  $S$  enclosing the airfoil [7]. The results of this calculation for a particular airfoil's simulation are displayed in Fig. 5. We rescale the computed forces by  $m\rho_\infty U_\infty \kappa$ , which corresponds to a *quantum of lift*: the ideal lift provided by a quantum of circulation.

The computed lift and drag are clearly not quantized. We attribute this to transient effects, in particular to the build-up of a dipolar density variation above and below the foil, as can be seen in the inset of Fig. 5(a). As discussed in the SI the density dipole, and the emitted and reflected density wave, lead to contributions to the lift and drag of the same order of magnitude as the two spikes seen in Fig. 5(a). To remove these effects we proceed as follows: far from the foil where speeds are low, we expect that the compressible piece,  $\mathbf{u}_C$ , of the velocity field will contain only density/sound waves. As detailed in the SI, the incompressible component of the velocity field  $\mathbf{u}_I \equiv \mathbf{u} - \mathbf{u}_C$ , is simply the sum of the ideal velocity field around the foil,  $\mathbf{u}_{\text{ideal}}$  and the velocity fields from the emitted vortices. Replacing  $\mathbf{u}$  with  $\mathbf{u}_I$  and using the density field prescribed by the steady Bernoulli equation, we recalculate the lift and drag and plot it in Fig. 5(b). Since this calculation differs from that of lift and drag on an airfoil in ideal fluid only in that we allowed the density  $\rho(u_I)$  to vary in space, it is not surprising that the lift is now quantized and the drag is nearly zero.

In conclusion we analysed the mechanisms responsible for vortex nucleation from an airfoil and its consequent acquired lift in a two-dimensional superfluid. On the one hand, we find results reminiscent of the classical theory of airfoils; with the emission of vortices at

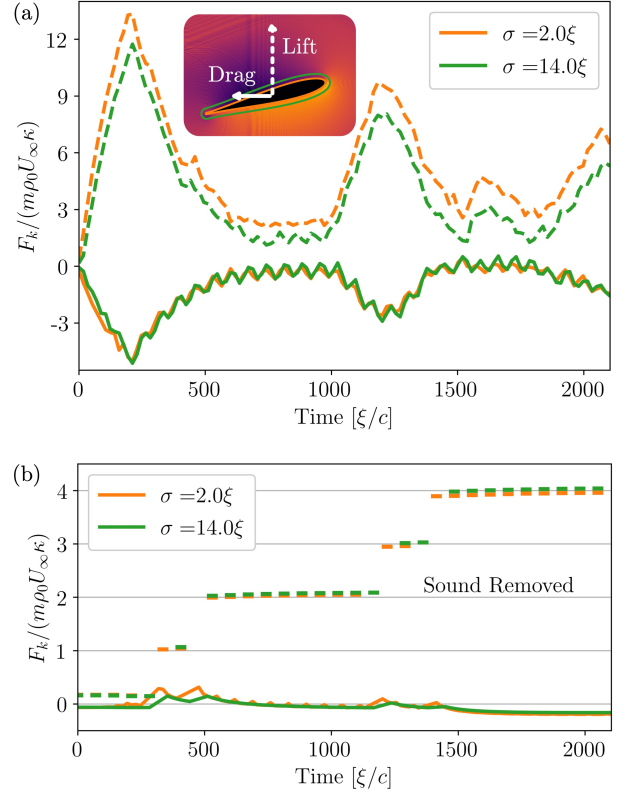


FIG. 5. Evolution of lift and drag: (a) Non-dimensional lift (dotted line) and drag (solid line) experienced by the airfoil throughout simulation with  $U_\infty = 0.29c$ ,  $L = 325\xi$ ,  $\alpha = 15.0^\circ$ , and  $\lambda = 0.1$ . Inset shows an exaggerated density field around the airfoil. Included are the integration contours for computing the force. (b) Non-dimensional lift (dotted line) and drag (solid line) experienced by the airfoil using  $\mathbf{u}_I$  and  $\rho(u_I)$ . A grid is overlaid to demonstrate the quantization of the lift, the steps coincide with vortex nucleation. Lift and drag were not computed on a contour if a vortex was within  $8\xi$ .

the trailing edge governed by the elimination of the singularity predicted by inviscid flow. On the other hand, a marked departure from classical flow is found in the stalling behavior. Accelerated hydrofoils and wings have recently been used to create vortices of arbitrary shape in classical fluids [26, 27], a technique which might generalize to superfluids, offering a potentially powerful new procedure in superfluid manipulation, vortex generation, and observation of quantized lift – a measurement originally attempted in  $^4\text{He}$  by Craig & Pellam [28] to demonstrate the quantization of circulation, later detected by Vinen using a different setup [29]. Among the various superfluid experimental realizations, some have recently started to address questions on vortex nucleation and manipulation using moving obstacles including cold atomic gases [21, 23, 30–33] and quantum fluids of light [34, 35]. Details of each experimental realization will differ: 3d effects need to be considered for non quasi-

two-dimensional BECs, the rotons' emission instead of vortex shedding might be important in  $^4\text{He}$ , and out-of-equilibrium exciton-polariton systems will require modelling to consider intrinsic forcing and damping terms. The time is right for superfluid flight!

---

\* Current address: Department of Physics, 77 Massachusetts Ave, Cambridge, MA 02139; swmusser@mit.edu

- [1] D. J. Acheson, in *Elementary Fluid Dynamics* (Oxford University Press, 1990) 1st ed., pp. 287–291.
- [2] J. D. Anderson Jr., *Fundamentals of Aerodynamics*, 5th ed. (McGraw-Hill Education, 2010).
- [3] P. K. Kundu, I. M. Cohen, and D. R. Dowling, in *Fluid Mechanics* (Elsevier Inc., 2016) 6th ed., pp. 820–879.
- [4] T. Frisch, Y. Pomeau, and S. Rica, *Physical Review Letters* **69**, 1644 (1992).
- [5] C. Huepe and M.-E. Brachet, *Physica D: Nonlinear Phenomena* **140**, 126 (1999).
- [6] B. Jackson, J. McCann, and C. Adams, *Physical Review Letters* **80**, 3903 (1997).
- [7] T. Winiecki, B. Jackson, J. F. McCann, and C. S. Adams, *Journal of Physics B: Atomic, Molecular and Optical Physics* **33**, 4069 (2000).
- [8] G. W. Stagg, N. G. Parker, and C. F. Barenghi, *Journal of Physics B: Atomic, Molecular and Optical Physics* **47** (2014), 10.1088/0953-4075/47/9/095304.
- [9] G. W. Stagg, A. J. Allen, C. F. Barenghi, and N. G. Parker, *Journal of Physics: Conference Series* **594** (2015).
- [10] T. Winiecki and C. S. Adams, *Europhysics Letters* **52**, 257 (2000).
- [11] C. Nore, C. Huepe, and M. Brachet, *Physical Review Letters* **84**, 2191 (1999).
- [12] Kazuki Sasaki, Naoya Suzuki, and Hiroki Saito, *Physical Review Letters* **104** (2010).
- [13] G. Stagg, N. Parker, and C. Barenghi, *Physical Review Letters* **118** (2017), 10.1103/PhysRevLett.118.135301.
- [14] D. Proment, M. Onorato, and C. F. Barenghi, *Physical Review E* **85** (2012), 10.1103/PhysRevE.85.036306.
- [15] D. Kleckner, L. H. Kauffman, and W. T. M. Irvine, *Nature Physics* **12**, 650 (2016).
- [16] C. Nore, M. Abid, and M. E. Brachet, *Physics of Fluids* **9**, 2644 (1997).
- [17] M. Kobayashi and M. Tsubota, *Physical Review Letters* **94** (2005), 10.1103/PhysRevLett.94.065302.
- [18] Natalia G. Berloff and Carlo F. Barenghi, *Physical Review Letters* **93** (2004).
- [19] Sergio Rica, in *Quantized Vortex Dynamics and Superfluid Turbulence*, Lecture Notes in Physics, Vol. 571, edited by C. F. Barenghi, R. J. Donnelly, and W. F. Vinen (Springer-Verlag Berlin Heidelberg, 2001) pp. 258–267.
- [20] G. A. El, A. M. Kamchatnov, V. V. Khodorovskii, E. S. Annibale, and A. Gammal, *Physical Review E* **80** (2009), 10.1103/PhysRevE.80.046317.
- [21] M. E. Mossman, M. A. Hoefer, K. Julien, P. G. Kevrekidis, and P. Engels, *Nature Communications* **9**, 4665 (2018).
- [22] Rica S. and Pomeau Y., in *Instabilities and Nonequilibrium Structures IV*, Mathematics and Its Applications No. 267 (Springer Dordrecht, 1993) 1st ed., pp. 351–364.
- [23] Woo Jin Kwon, Joon Hyun Kim, Sang Won Seo, and Y. Shin, *Physical Review Letters* **117** (2016).
- [24] These images are from the National Committee for Fluid Mechanics Films: Vorticity, Part 2 and Fundamentals of Boundary Layers, copyright 1961 Education Development Center, Inc. Used with permission with all other rights reserved.
- [25] For a better estimation of the healing layer one should in principle extend the expansion to higher order, as suggested for instance in [5] for a cylinder uniformly moving in a superfluid.
- [26] D. Kleckner and W. T. Irvine, *Nature Physics* **9**, 253 (2013).
- [27] M. W. Scheeler, W. M. van Rees, H. Kedia, D. Kleckner, and W. T. Irvine, *Science* **357**, 487 (2017).
- [28] P. P. Craig and J. R. Pellam, *Phys. Rev.* **108**, 1109 (1957).
- [29] W. F. Vinen, *Proceedings of the Royal Society A* **260**, 218 (1961).
- [30] N. Meyer, H. Proud, M. Perea-Ortiz, C. O’Neale, M. Baumert, M. Holynski, J. Kronjger, G. Barontini, and K. Bongs, *Physical Review Letter* **119** (2017), 10.1103/PhysRevLett.119.150403.
- [31] A. Burchianti, F. Scazza, A. Amico, G. Valtolina, J. Seman, C. Fort, M. Zaccanti, M. Inguscio, and G. Roati, *Physical Review Letters* **120** (2018), 10.1103/PhysRevLett.120.025302.
- [32] J. W. Park, B. Ko, and Y. Shin, *Physical Review Letters* **121** (2018), 10.1103/PhysRevLett.121.225301.
- [33] C. Michel, O. Boughdad, M. Albert, P.-. Larr, and M. Bellec, *Nature Communications* **9**, 2108 (2018).
- [34] A. Amo, S. Pigeon, D. Sanvitto, V. G. Sala, R. Hivet, I. Carusotto, F. Pisanello, G. Lemnager, R. Houdr, E. Giacobino, C. Ciuti, and A. Bramati, *Science* **332**, 1167 (2011).
- [35] D. Vocke, K. Wilson, F. Marino, I. Carusotto, E. M. Wright, T. Roger, B. P. Anderson, P. Öhberg, and D. Faccio, *Physical Review A* **94** (2016), 10.1103/PhysRevA.94.013849.